



Antioxidant activity of silver nanoparticles synthesized from *Tagetes erecta* L. leaves

Ramazan ERENLER^{1,*}, Esmâ Nur GEÇER¹, Nusret GENÇ¹, Dürdane YANAR²

¹Department of Chemistry, Faculty of Arts and Sciences, Tokat Gaziosmanpaşa University, 60250 Tokat, Turkey

²Department of Plant Protection, Faculty of Agriculture, Tokat Gaziosmanpaşa University, 60250 Tokat, Turkey

Received: 6 October 2021; Revised: 30 October 2021; Accepted: 10 November 2021

*Corresponding author e-mail: erenler@gmail.com

Citation: Erenler, R.; Geçer, E. N.; Genç, N.; Yanar, D. *Int. J. Chem. Technol.* 2021, 5 (2), 141-146.

ABSTRACT

Tagetes erecta leaves were extracted with deionized water at 55°C for around 3.0 hours and filtered. After removing of water from a quantity of solution by a rotary evaporator, the crude extract was obtained. The other filtrate was reacted with silver nitrate solution at 65°C for 2.5 hours to produce the silver nanoparticles (te-AgNPs). The structure of te-AgNPs was characterized by spectroscopic study. The characteristic hydroxyl vibrational of te-AgNPs was observed at 3214 cm⁻¹ in the Fourier Transform-Infrared Spectroscopy (FTIR). The maximum absorption was observed at 422 nm by Ultraviolet-Visible (UV-Vis) spectrophotometer. Scanning Electron Microscope (SEM) spectrum also proved the desired product with an average size of 46.26 nm. X-Ray Diffraction (XRD) spectrum revealed the te-AgNPs to be face-centered cubic crystalline structures. Antioxidant activity tests of extract and te-AgNPs were carried out and te-AgNPs displayed the significant antioxidant activity with the IC₅₀ values of 23.80 µg/mL, 4.46 µg/mL, and 2.79 µmol/mg sample corresponded to the 2,2-Diphenyl-1-picrylhydrazyl (DPPH), 2,2'-Azinobis(3-ethylbenzothiazoline-6-sulfonic acid) (ABTS) and Ferric ion Reducing Antioxidant Power) (FRAP) activities respectively.

Keywords: *Tagetes erecta* leaves, nanoparticles, spectroscopy, natural products, antioxidant activity.

1. INTRODUCTION

Aromatic and medicinal plants play a significant function in drug development as they contain bioactive compounds called secondary metabolites.¹⁻⁴

Nanotechnology includes the physicochemical and biological process to construct nanomaterials, which are less than 100 nm and have unique properties.⁵

Tagetes erecta yapraklarından sentezlenen nanopartiküllerin antioksidan aktivitesi

ÖZ

Tagetes erecta yaprakları yaklaşık saf su ile 55°C de 3.0 saat ısıtıldı ve daha sonra filtre edildi. Ham özüt elde etmek için süzölmüş çözeltinin bir miktarının çözücüsü döner buharlaştırıcı ile uzaklaştırıldı. Diğer filtre edilmiş çözelti, gümüş nitrat çözeltisi ile 65°C da 2.5 saat etkileştirilerek gümüş nanopartiküller (te-AgNPs) elde edildi. te-AgNPs yapısı spektroskopik yöntemlerle aydınlatıldı. te-AgNPs'in karakteristik hidroksil titreşimi, Fourier Transform Infrared Spektroskopisi (FTIR) spektrumunda 3214 cm⁻¹ de gözlemlendi. Ultraviolet-Visible (UV-Vis) spektrofotometre ile maksimum absorpsiyon 422 nm de gözlemlendi. Taramalı Elektron Mikroskop (SEM) spektral analizi ile de istenilen ürünün ortalama büyüklüğü 46.26 nm olarak belirlendi. X-Işını Kırınımı (XRD) spektrumu, te-AgNPs'in yüzey merkezli kübik kristal yapısında olduğunu ortaya koydu. Özüt ve te-AgNPs örneklerinin antioksidan aktivite testleri yapıldı ve te-AgNPs örneği, 23.80 µgml⁻¹, 4.46 µgml⁻¹, ve 2.79 µmolmg⁻¹ örnek⁻¹, IC₅₀ değerleri ile sırasıyla önemli derecede 2,2-Difenil-1-pikrilhidraliz (DPPH), 2,2'-azinobis(3-etilbenzotiazolin-6-sulfonat) (ABTS) ve İndirgeyici Antioksidan Gücü (FRAP) aktivitesi gösterdi.

Anahtar Kelimeler: *Tagetes erecta* yapraklar, nanopartikül, spektroskopi, doğal ürünler, antioksidan aktivite.

Nanotechnology has been used extensively in various fields such as nanomedicines, biomaterials, nanoelectronics, imaging, agriculture, environmental In medicine, it has been widely employed for diagnosis, and treatment of diseases, as well as drug delivery, and novel drug formulations.⁶ Therefore, the synthesis of nanoparticles has attracted great interest and many synthesis pathways have been developed such as photochemical, radiation and electrochemical. Yet, the

corresponding methods cause pollution, toxicity and require drastic reaction conditions. So, natural products mediated synthesis of nanoparticles has opened a new era to this research area, since this method is eco-friendly, economical, and provides high efficiency with scale-up. Natural products like pure compounds, plant extracts, algae, enzymes, vegetable wastes, seaweed, arthropods have been used for nanoparticles production.⁷ Natural products mediated synthesized nanoparticles displayed considerable biological actions such as anticancer, antioxidant, anti-inflammatory, antibacterial, antifungal, antiviral, acetylcholinesterase, mosquito larvicidal, photocatalytic.⁸⁻¹¹

Tagetes genus belongs to Asteraceae family and includes 122 species. *Tagetes erecta* Linn. is an ornamental flower that is well-known as Marigold.¹² The corresponding plant has been employed as a traditional medicine for the therapy of colds, rheumatism, and bronchitis. Moreover, the juice of this plant has sudorific, vomitive, febrifuge, vermifuge, emetic properties. *Tagetes erecta* consists of lutein, xanthophyll.¹³ Lutein is the responsible compound for the coloring of the *T. erecta*.¹⁴ Besides, it has a protective effect against macular degeneration disease, cardiovascular disease, cancer, oxidative effects. The flower of *T. erecta* was reported to have anti-inflammatory, antimutagenic, antiviral, and antitumor effects.^{15,16}

Reactive oxygen species are called free radicals that are essential for many reactions in the eukaryotic cell.¹⁷ In some conditions like smoking, drugs, alcohol, bad lifestyle, excess free radicals are produced that harm to the lipid, protein, and nucleic acid leading to the diseases such as cancer, Alzheimer, and diabetes. Therefore, many antioxidant-based drugs, as well as food supplement containing antioxidant compounds, have been developed to combat the corresponding challenge.¹⁸ Antioxidants are essential not only for humans but also to prevent food from spoiling.¹⁹ Throughout the storage and dealing out of foods, lipids oxidation like enzymatic and auto oxidations are the main reactions that lead to food deterioration affecting the color, smell, taste, and nutritional value of foods. Hence, antioxidants are used for food to prevent radicalic reactions.²⁰ Synthetic antioxidants, such as butylated hydroxyl toluene (BHT) and butylated hydroxyl anisole (BHA) which are commonly used for food are restricted due to their toxic effect and possible carcinogens.²¹ Therefore, the interest in natural antioxidants has been increased considerably by consumer preference and industries.²²

Since the silver atoms are encapsulated and stabilized by bioactive compounds of the plants, the interest in nanoparticles for biological effects has been increased steadily. The nanoparticles using the medicinal plants were reported to display significant antioxidant activity.²³

Herein, silver nanoparticles (te-AgNPs) were synthesized using *T. erecta* leaves and their structure was characterized by spectroscopic methods. Moreover, their antioxidant activity was accomplished using the DPPH[•] scavenging, ABTS^{•+} radical cation scavenging, and reducing power assays.

2. MATERIALS AND METHODS

2.1. General

All chemicals and solvents utilized in nanoparticles synthesis and antioxidant activity tests were supplied from E. Merch (Darmstadt, Germany).

2.2. Plant material

Tagetes erecta L., a well-known plant was collected from the university campus during the maturation stage in August 2020.

2.3. Green synthesis of silver nanoparticles

Tagetes erecta leaves (40 g) was extracted with deionized water (500 mL) for 3 hours at 55°C. The solution was double filtered and divided equally into two pieces for crude extract and te-AgNPs. One solution (250 mL) was subjected to a rotary evaporator to produce crude extract (2.0 g). Another solution was used for the synthesis of te-AgNPs. *T. erecta* (250 mL) solution was reacted with AgNO₃ dissolved in deionized water (0.071 M, 100 mL) for 2.5 hours at 65°C. After the centrifugation at 4000 rpm for 15 min, silver nanoparticles were obtained, washed and lyophilized (0.75 g)²⁴ (Figure 1).

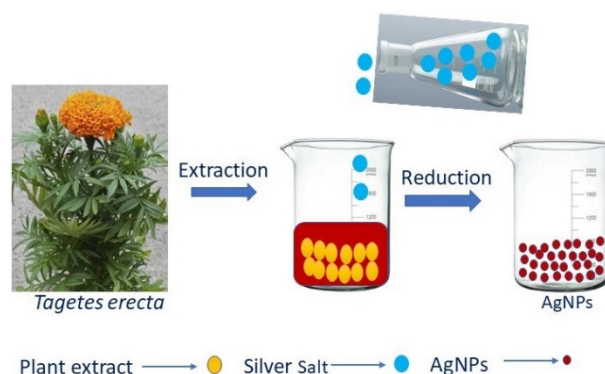


Figure 1. The green synthesis of te-AgNPs.

2.4. Characterization of silver nanoparticles

The structural elucidation of synthesized silver nanoparticles was carried out by fully spectroscopic analyses. Ultraviolet-visible, UV-2600 spectrophotometer was used to determine of maximum absorption of silver nanoparticles as well as antioxidant activity analyses. The functional groups of compounds that capped to the silver as well as stabilized the silver

was determined by Fourier to transform infra-red, FTIR 4700 spectrometer. X-ray diffraction (XRD) analysis was executed by Empyrean, Malvern Panalytical diffractometer. The diffracted intensity was recorded in the 2θ region ranging from 20° to 90° . Scanning Electron Microscope (SEM) analysis was carried out by Quanta Feg450 and elemental analysis was operated by EDAX detector and EDX.

2.5. Antioxidant activity

2.5.1. DPPH[•] free radical scavenging assay

DPPH[•] scavenging effect was carried out by the method described in literature.² Firstly, stock solutions (1 mg/mL) of extract and te-AgNPs were prepared. Each stock solution (20, 40, and 80 μ L) was completed to 3.0 mL with ethanol. DPPH[•] solution in ethanol (1.0 mL, 0.26 mM) was added to each solution. After the vortex process, the solution was incubated for 30 minutes at room temperature (rt), then absorbance measurement was executed with a spectrophotometer at 517 nm. The results were calculated as IC₅₀.²⁵

2.5.2. ABTS^{•+} radical cation assay

The treatment of ABTS solution (2.0 mM) with the sodium persulfate (2.45 mM) yielded the ABTS^{•+} which was kept in dark for 5 h at rt. ABTS^{•+} solution was treated with sodium phosphate buffer (0.1 mM, pH 7.4). The sample (te-AgNPs and extract) was reacted with ABTS^{•+} at various concentrations. The absorbance measurement was performed at 734 nm. The results were given as IC₅₀.²⁶

2.5.3. Ferric reduction antioxidant power (FRAP) assay

FRAP activity test was executed by the reported work.²⁷ The analyte (100 μ L, 40-150 μ g/mL) was mixed with the phosphate buffer (1.15 mL, 0.20 M, pH 6.7), potassium ferric cyanide (1.0%, 1.25 mL) and the mixture was incubated for 25 min at 55°C , later FeCl₃ (0.25 mL, 0.1%), and CCl₃COOH (1.25 mL, 10%) were added. After the vortex process for 5 min absorbance measurement was executed on a spectrophotometer (700 nm).

2.6. Statistical analysis

The statistical analysis of antioxidant activity was carried out using GraphPad Prism (version 8.00) with one-way ANOVA software. The results were expressed as mean values \pm standard deviation ($P < 0.05$).

3. RESULTS AND DISCUSSION

3.1. Synthesis and UV-Vis spectral analysis of silver nanoparticles

te-AgNPs were synthesized using *T. erecta* leaves. Due to the medicinal importance of *Tagetes* species, te-AgNPs capped by secondary metabolites of *T. erecta* could be a valuable reagent for the food and drug development industry. The color change from yellow to dark brown proved the biosynthesis of te-AgNPs (Figure 2).

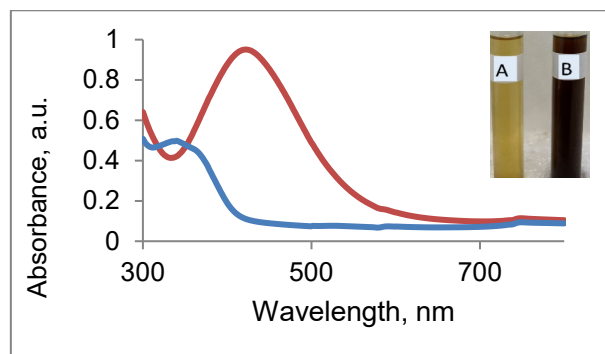


Figure 2. Aqueous solution of extract (A), te-AgNPs (B) and UV-Vis spectrum of extract (A) and te-AgNPs (B) at 422 nm.

The absorption in the visible region ranging from 350 to 550 nm revealed the formation of AgNPs.²⁸ AgNPs synthesized from *T. erecta* have an absorption peak at 422 nm, which also verifies the structure of te-AgNPs. Ag⁺ ions were reduced by the secondary metabolites of *T. erecta*. After the reduction, clustering, and growth, the nanoparticles formed (Figure 3). The oxidation and reduction reaction of *T. erecta* leaves solution with silver nitrate solution at 60°C yielded the silver nanostructure formation. Since *T. erecta* consisted of quercetin,²⁹ a reaction mechanism was showed with this compound.

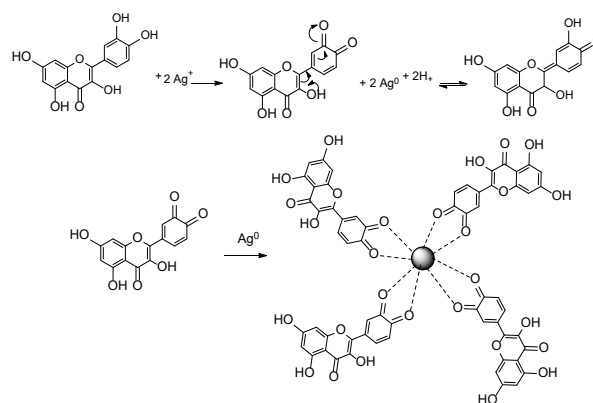


Figure 3. Plausible reaction mechanism of synthesis of te-AgNPs.

3.2. Fourier-transform infrared spectroscopy

FTIR spectroscopy presented the bioactive compounds in charge of the reduction of Ag⁺ ions and the effective stabilization of te-AgNPs synthesized by the corresponding plant. FTIR spectral analyses of extract and te-AgNPs were performed and a slight difference

between extract and te-AgNPs spectrum confirmed the formation of te-AgNPs (Figure 4). The vibrational signal at 3305 cm⁻¹ represented the OH of the flavonoid rings. CH stretching vibrational signals of alkanes appeared at 2973 cm⁻¹ and 2885 cm⁻¹. The peak at 1574 cm⁻¹ corresponded to the double bond of an alkene. The vibrational signal at 1381 could be due to the CH bending of alkane. The signals observed at 1085 cm⁻¹, 1047 cm⁻¹, and 880 cm⁻¹ represented the CN stretching of amine, CN stretching of amine, and C=C bending of alkene respectively. The signals that appeared at 512 cm⁻¹ and 428 cm⁻¹ could be due to the silver oxide which accorded to the reported work.³⁰ Ag⁺ ions might be reduced to Ag⁰ by the secondary metabolites of plant extract, and consequently, the green synthesized AgNPs were capped and stabilized by functional groups of corresponding metabolites.³¹

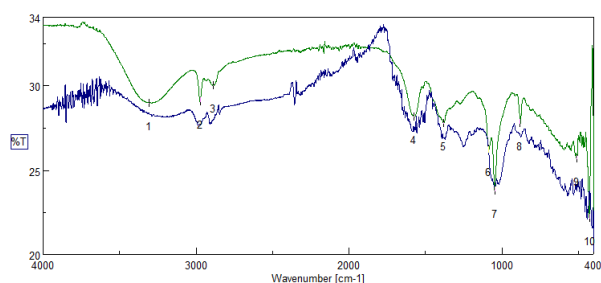


Figure 4. FTIR spectrum of extract (A) and AgNPs (B), 1: 3305, 2: 2973, 3: 2885, 4: 1574, 5: 1381, 6: 1085, 7: 1047, 8: 880, 9: 512, 10: 428

3.3. X-ray diffraction

The crystalline nature of te-AgNPs was determined by XRD analysis. Diffraction peaks at 2θ values of 38.1°, 44.3°, 64.4°, and 77.4° corresponded to the (111), (200), (220), and (311) reflections of the face-centered cubic crystalline (fcc) structure which was in accordance with the standard silver card values (JCPDS No. 87-0720). A previous study also confirmed the structure.³² Debye-Scherrer formula was used for calculation of average crystalline size (1)

$$D = 0.9 \lambda / \beta \cos \theta \quad (1)$$

D represents the average crystalline size (°A), λ designates the x-ray wavelength (nm), β describes the angular line with at half maximum intensity (radians) and θ is the angle (degree). The sharp diffraction peak in the XRD pattern displayed the crystalline properties of te-AgNPs. The impurity diffraction peaks were caused by the plant materials. The particle size was calculated as 46.26 nm (Figure 5).

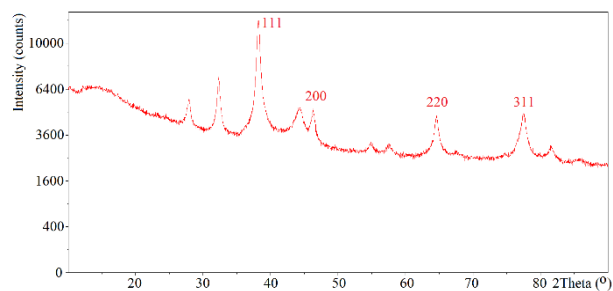


Figure 5. XRD pattern of te-AgNPs synthesized

3.4. Scanning Electron Microscope

The morphology of green synthesized te-AgNPs was presented by SEM analysis (Figure 6). SEM image revealed the dispersion of agglomerated clusters that were distributed over the surface. The energy dispersive analysis (EDX) verified the presence of NPs. Furthermore, the notable strong peak of Ag in synthesized NPs in the EDX spectrum at around 3 and 3.3 keV approved the structure of synthesized nanoparticles. In addition, elemental analysis proved the proposed structure as well (Figure 7).

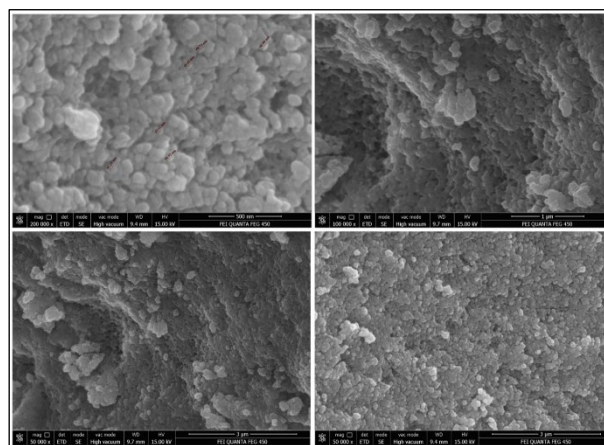


Figure 6. SEM images of te-AgNPs

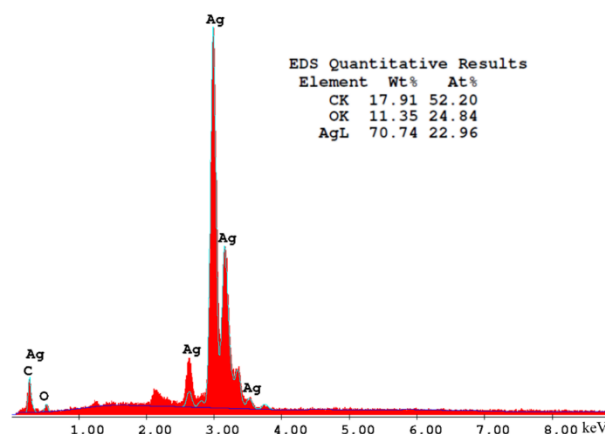


Figure 7. EDX spectrum and elemental analysis of te-AgNPs.

3.5. Antioxidant activity

Antioxidant activity of extract and silver nanoparticles from *T. erecta* leaves was achieved using DPPH, ABTS⁺ and FRAP assays (Figure 8). In DPPH assay, AgNPs (23.8 µg/mL, IC₅₀) revealed a higher effect than that of the extract (40.0 µg/mL, IC₅₀) significantly. Yet, their radical scavenging effects were lower than the standards. In concerning the ABTS assay, AgNPs revealed excellent activity (4.5 µg/mL, IC₅₀), even better than the standards BHT (7.3 µg/mL, IC₅₀), and Trolox (5.7 µg/mL, IC₅₀). However, the extract exhibited moderate activity (19.3 µg/mL, IC₅₀). The same trend was observed in the FRAP assay. In FRAP assay, the effect of te-AgNPs (2.8 µmol TE/mg extract) was found higher than that of the extract (0.8 µmol TE/mg extract). Hence, te-AgNPs synthesized from *T. erecta* could be a promising antioxidant agent for the food and pharmaceutical industries. AgNPs synthesized from *T. erecta* was reported to have antibacterial activity against *Escherichia coli*, *Staphylococcus aureus* bacteria.³³ Moreover, AgNPs synthesized from *T. erecta* revealed improved photodegradation of Rhodamine B dye.³⁴ Nickel oxide nanoparticles prepared using *T. erecta* leaf extract exhibited significant photocatalytic, antibacterial activities as well as high sensitivity for glucose sensors.^{35,36} te-AgNPs synthesized from *T. erecta* revealed the DPPH free radical scavenging effect, only DPPH assay was used for antioxidant activity and silver nanoparticles were synthesized at room temperature. Moreover, *T. erecta* was collected from India for the corresponding study.³⁷ However, in our study, *T. erecta* was collected in Tokat, DPPH, ABTS and FRAP assays were carried out for the antioxidant activity. Moreover, silver nanoparticles were synthesized at 65 °C. Silver nanoparticles synthesized from *T. erecta* leaves were reported to enhance the plant growth.³⁸ Another research presented that the AgNPs obtained from *T. erecta* leaves extract displayed the wound healing activity and anti-inflammatory activity in female Wistar albino rats.³⁹ In addition, Silver nanoparticles synthesized from *T. erecta* were reported to display supercapacitor and electrochemical sensing applications,⁴⁰ and amoxicillin detection.⁴¹

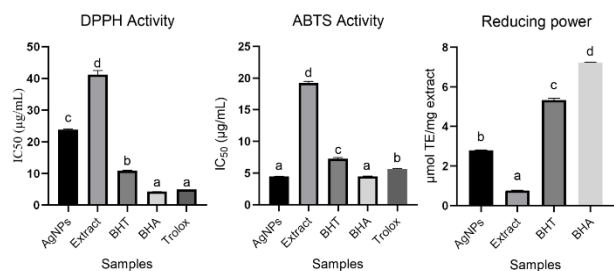


Figure 8. Antioxidant activity of te-AgNPs and extract. The results were reported as mean values \pm SDs of three independent assays ($P < 0.05$). Values followed by the different letter are significantly different.

4. CONCLUSION

The synthesis of silver nanoparticles is one step, cheap, eco-friendly, and scale-up. The te-AgNPs synthesized from *T. erecta* leaves could be a promising material for the antioxidant agent. *T. erecta* includes significant bioactive compounds. Thus, the silver capped and stabilized by these compounds could be considered an effective material for the pharmaceutical and food industries. In other words, te-AgNPs synthesized from *T. erecta* are a promising agent that may offer a significant application in the treatment of oxidative stress-related diseases.

Conflict of interest

The authors declare that *there is no a conflict of interest with any person, institute, company, etc.*

REFERENCES

- Topçu, G.; Erenler, R.; Çakmak, O.; Johansson, C. B.; Çelik, C.; Chai, H.-B.; Pezzuto, J. M. *Phytochemistry* **1999**, 50 (7), 1195-1199.
- Elmastas, M.; Ozturk, L.; Gokce, I.; Erenler, R.; Aboul-Enein, H. Y. *Anal Lett* **2004**, 37 (9), 1859-1869.
- Demirtas, I.; Erenler, R.; Elmastas, M.; Goktasoglu, A. *Food Chem* **2013**, 136 (1), 34-40.
- Sahin Yaglioglu, A.; Akdulum, B.; Erenler, R.; Demirtas, I.; Telci, I.; Tekin, S. *Med Chem Res* **2013**, 22 (6), 2946-2953.
- Rama Krishna, A.; Espenti, C.; Rami Reddy, Y.; Obbu, A.; Satyanarayana, M. *J Inorg Organomet Polym Mater* **2020**, 30, 4155-4159.
- Aiswariya, K.; Jose, V. *J Inorg Organomet Polym Mater* **2021**, 31, 3111-3124.
- Lateef, A.; Ojo, S. A.; Elegbede, J. A. *Nanotechnol Rev* **2016**, 5 (6), 601-622.
- Bachheti, R. K.; Fikadu, A.; Bachheti, A.; Husen, A. *Saudi J Biol Sci* **2020**, 27 (10), 2551.
- Vanaraj, S.; Keerthana, B. B.; Preethi, K. *J Inorg Organomet Polym Mater* **2017**, 27 (5), 1412-1422.
- Erenler, R.; Dag, B. *Inorg Nano-Met Chem* **2021**, <https://doi.org/10.1080/24701556.2021.1952263>.
- Ravindra, S.; Mulaba-Bafubandi, A. F.; Rajinikanth, V.; Varaprasad, K.; Reddy, N. N.; Raju, K. M. *J Inorg Organomet Polym Mater* **2012**, 22 (6), 1254-1262.

12. Jiang, M.; Xu, Y.; Wang, L.; Liu, J.; Yu, J.; Chen, H. *Mitochondrial DNA Part B* **2020**, 5 (3), 2966-2971.
13. Hojnik, M.; Škerget, M.; Knez, Ž. *LWT-Food Science and Technology* **2008**; 41(10): 2008-2016.
14. Gau, W.; Ploschke, H.-J.; Wünsche, C. *J Chromatogr A* **1983**, 262, 277-284.
15. Chitrakar, B.; Zhang, M.; Bhandari, B. *Trends Food Sci Technol* **2019**, 89, 76-87.
16. Gansukh, E.; Mya, K. K.; Jung, M.; Keum, Y.-S.; Kim, D. H.; Saini, R. K. *Food Chem Toxicol* **2019**, 127, 11-18.
17. Erenler, R.; Sen, O.; Aksit, H.; Demirtas, I.; Yaglioglu, A. S.; Elmastas, M.; Telci, İ. *J Sci Food Agr* **2016**, 96 (3), 822-836.
18. Erenler, R.; Adak, T.; Karan, T.; Elmastas, M.; Yildiz, I.; Aksit, H.; Topcu, G.; Sanda, M. A. *The Eurasia Proceed Sci Tech Eng Math* **2017**, 1, 139-145.
19. Erenler, R.; Meral, B.; Sen, O.; Elmastas, M.; Aydin, A.; Eminagaoglu, O.; Topcu, G. *Pharm Biol* **2017**, 55 (1), 1646-1653.
20. Guzel, A.; Aksit, H.; Elmastas, M.; Erenler, R. *Pharmacogn Mag* **2017**, 13 (50), 316-320.
21. Sasaki, Y. F.; Kawaguchi, S.; Kamaya, A.; Ohshita, M.; Kabasawa, K.; Iwama, K.; Taniguchi, K.; Tsuda, S. *Mutat Res Genet Toxicol Environ Mutagen* **2002**, 519 (1-2), 103-119.
22. Elmastas, M.; Celik, S. M.; Genc, N.; Aksit, H.; Erenler, R.; Gulcin, İ. *Int J Food Prop* **2018**, 21 (1), 374-384.
23. Burlacu, E.; Tanase, C.; Coman, N.-A.; Berta, L. *Molecules* **2019**, 24 (23), 4354.
24. Genc, N.; Yildiz, I.; Chaoui, R.; Erenler, R.; Temiz, C.; Elmastas, M. *Inorg Nano-Met Chem* **2021**, 51 (3), 411-419.
25. Erenler, R.; Yilmaz, S.; Aksit, H.; Sen, O.; Genc, N.; Elmastas, M.; Demirtas, I. *Rec Nat Prod* **2014**, 8 (1), 32-36.
26. Erenler, R.; Telci, İ.; Ulutas, M.; Demirtas, I.; Gul, F.; Elmastas, M.; Kayir, O. *J Food Biochem* **2015**, 39 (5), 622-630.
27. Elmastaş, M.; Telci, İ.; Aksit, H.; Erenler, R. *Turk J Biochem* **2015**, 40 (6), 456-462.
28. Zuas, O.; Hamim, N.; Sampora, Y. *Mater Lett* **2014**, 123, 156-159.
29. Lu, H.; Yang, S.; Ma, H.; Han, Z.; Zhang, Y. *Anal Methods* **2016**, 8 (15), 3255-3262.
30. Iftikhar, M.; Zahoor, M.; Naz, S.; Nazir, N.; Batiha, G. E.-S.; Ilaq, R.; Bari, A.; Hanif, M.; Mahmood, H. M. *J Nanomater* **2020**, ID 8949674, <https://doi.org/10.1155/2020/8949674>.
31. Gecer, E. N.; Erenler, R.; Temiz, C.; Genc, N.; Yildiz, I. *Particul Sci Technol* **2021**, <https://doi.org/10.1080/02726351.2021.1904309>.
32. Beyene, H. D.; Werkneh, A. A.; Bezabh, H. K.; Ambaye, T. G. *Sust Mat Technol* **2017**, 13, 18-23.
33. Maji, A.; Beg, M.; Das, S.; Aktara, M. N.; Nayim, S.; Patra, A.; Islam, M. M.; Hossain, M. *Process Biochem* **2020**, 97, 191-200.
34. Katta, V.; Dubey, R. *Mat Today Proceed* **2021**, 45, 794-798.
35. Maji, A.; Beg, M.; Das, S.; Aktara, M. N.; Nayim, S.; Patra, A.; Islam, M. M.; Hossain, M. *Process Biochem* **2020**, 97, 191-200.
36. Likasari, I. D.; Astuti, R. W.; Yahya, A.; Isnaini, N.; Purwiandono, G.; Hidayat, H.; Wicaksono, W. P.; Fatimah, I. *Chem Phys Lett* **2021**, 780, 138914.
37. Tyagi, P. K.; Tyagi, S.; Gola, D.; Arya, A.; Ayatollahi, S. A.; Alshehri, M. M.; Sharifi-Rad, J. *J Nanomater* **2021**, 2021, ID 6515419.
38. Kumar, P.; Pahal, V.; Gupta, A.; Vadhan, R.; Chandra, H.; Dubey, R. C. *Sci. Rep.* **2020**, 10 (1), 20409.
39. Selvam, S. I.; Joicesky, S. M. B.; Dashli, A. A.; Vinothini, A.; Premkumar, K. *J Appl Nat Sci* **2021**, 13 (1), 343-351.
40. Salve, M.; Mandal, A.; Amreen, K.; Pattnaik, P. K.; Goel, S. *Microchem J* **2020**, 157, 104973.
41. ul Ain, N.; Anis, I.; Ahmed, F.; Shah, M. R.; Parveen, S.; Faizi, S.; Ahmed, S. *Sens Actuators B Chem* **2018**, 265, 617-624.